RHAPSODY: Reconstructing Hankel rAdial Profiles in centro-Symmetric Objects with Discrete rings for astrophYsics

Julien Drevon, Florentin Millour, Pierre Cruzalèbes, Peter Scicluna, Claudia Paladini

HAL Id: hal-03806294
https://cnrs.hal.science/hal-03806294

Submitted on 19 Oct 2022

RHAPSODY: Reconstructing Hankel rAdial Profiles in centro-Symmetric Objects with Discrete rings for astrophYsics

Julien Drevon[a,b], Florentin Millour[a], Pierre Cruzalebes[a], Peter Scicluna[b], and Claudia Paladini[b]

[a]Université Côte d'Azur, Observatoire de la Côte d'Azur, CNRS, Laboratoire Lagrange, France
[b]European Southern Observatory, Alonso de Córdova, 3107 Vitacura, Santiago, Chile

ABSTRACT

RHAPSODY is an intensity profile reconstruction code built to handle 2D centro-symmetric structures using interferometric data. RHAPSODY has been built to provide the community with a code requiring less parameters than classical image reconstruction code. This has as consequence leading to less solution non-uniqueness problems, a better convergence, and a better dynamic range assuming a centro-symmetric source at all wavelengths. RHAPSODY main steps are organized as following: In the first place, at each wavelengths, the code build a unique 1D structure made of concentric discrete uniform rings. Then, it applies the Hankel transform to reconstruct the equivalent visibility profile. Next, a change of coordinate is used on the 1D visibility profile to simulate the inclination and the rotation of the structure in the 2D Fourier plane. After a fitting process on the interferometric observations based on a χ^2 and Bayesian method, RHAPSODY apply an inverse Fourier transform and reconstruct the equivalent structure in the 2D image plane.
According to preliminary tests made on RHAPSODY, the code is able to well reproduce 1D and 2D centro-symmetric structures up to a dynamic range of 0.5%.

Keywords: SPIE Proceedings, image reconstruction, intensity profile, astronomical objects

1. INTRODUCTION

Image Reconstruction (IR) for long-baseline interferometry has been in the past a real challenge, that is still an active research topic today. An interferometer measures the amplitude and phase of the complex degree of coherence of the incoming light, meaning that in principle a straightforward inverse Fourier transform of interferometric data would enable one to get an image of the observed astrophysical object. However, this is not possible in practice because of several issues: an interferometer provides an uneven sampling of the data, leading to information voids ; it provides a non-linear way of making available the measures (amplitude and phase), leading to a non-convex problem ; finally an image contains a number of information (pixel intensities) that outperform by a large fraction the limited number of measurements, leading to a non-unique solution. Solving the IR problem in interferometry is therefore solving a non-convex inverse problem in a sparse case. Thanks to innovative ideas like the use of a Bayesian approach combined with maximum entropy[1] or various other regularizations,[2] plus an efficient weighting and grid-search,[3] self-calibration,[4] and more recently the emergence of machine learning,[5] IR has become possible with long-baseline interferometry.

Yet, IR is still of a difficult access for the general user, because mainly of the non-unicity of the solution, and the hand-tweaking of parameters to solve the IR problem (albeit it has been made available, e.g. with oi-imaging). One way to tackle these issues is to reduce by a large fraction the number of input parameters to the inverse problem, either by considering the imaging problem intrinsically sparse,[6] or by radically changing the IR paradigm.

RHAPSODY is a proposition for the second assertion: instead of reconstructing an image, this tool proposes to reconstruct radial profiles.

Further author information:
Julien Drevon: E-mail: julien.drevon@oca.eu, Telephone: +33 (0)6 11 93 42 86

This makes it a very complementary tool to already existing image reconstruction software. The aims of this code is to provide a fast and robust geometrical description of an astrophysical environment with a centro-symmetric model. We adopt a 1D Hankel transform combined with a Bayesian approach to reconstruct the radial intensity profile of the source. The Hankel transform has the advantage of requiring less parameters than classical image reconstruction techniques, reducing the non-unicity of solutions, improving convergence, and providing a better dynamic range.

In Section 2 we present step by step the RHAPSODY tool and its features to get an insight in the core of the code and the process involved in the "image" reconstruction. Next, in Section 3 we discuss the robustness of the RHAPSODY outputs thanks to simulated interferometric data and we estimate its intrinsic dynamic range. Then, finally we show in Section 4 some examples of RHAPSODY applied to real or simulated interferometric data.

2. THE RHAPSODY TOOL AND FEATURES

RHAPSODY * can handle interferometric data that are stored in the standard OIFITS format.[7] In this section we will go through all the important steps of the software.

2.1 Setting the initial parameters

The important initial parameters are only a few. We can separate them in 3 different categories: i) facilitate the work of reading OIFITS files, ii) init the model structure, iii) define the fitting method.

To facilitate the work of reading OIFITS files, RHAPSODY needs as input the number of telescope involved in the observations. Furthermore, in order to avoid the presence of unexpected correlated flux among the OI_VIS and OI_VIS2 table, the user needs to precise if the FLUX table is expected in the data. If not, we assume that in absence of the FLUX table, the OI_VIS and OI_VIS2 tables contain visibilities and squared visibilities, respectively. In the case where several bands are present in the OIFITS file, the user need to provide the names and the wavelengths intervals in which he wants to do the image reconstruction.

To initialize the model structure, RHAPSODY needs the initial intensity profile as well as the number of rings and their respective angular diameter (see Section 2.2 for details). Up to now, the user can only chose among the Gaussian, Uniform Disk, or power-law profiles as initial guess.

Finally, to define the fitting method, RHAPSODY needs the following inputs: the desired regularization (between the Total Variation and the Quadratic Smoothness, see Section 2.3 for details), the value of the hyper-parameter to use (a list of hyper-parameter values can be provided), the fitting method (by default COBYLA), as well as the tolerance and the maximum of iterations to converge to a solution (the computation time is very sensitive to the tolerance).

2.2 Rings and Hankel Profile

Instead of forcing the routine to describe a given component (for example the dust envelope) with a particular geometrical model (for example a Gaussian disk), we use a large number of concentric uniform narrow rings (of width given as an input) to reproduce the radial profile of the stellar environment. With this method, thick rings are reproduced by contiguous narrow rings. This Hankel profile is built thanks to a set of N_{step} concentric circular rings with diameters $\theta_k = k\theta_0$, where $\theta_0 = 0.5\lambda/B$ being selected as a fraction of the angular resolution of the interferometer. Within that assumption, we write the normalized monochromatic radial profile as:

$$I_{\text{Hankel}}[h_k(\lambda)] = \frac{4}{\pi} \sum_{k=0}^{N_{\text{step}}-1} h_k(\lambda) \; \frac{\Pi(\theta_{k+1}) - \Pi(\theta_k)}{\theta_{k+1}^2 - \theta_k^2} \tag{1}$$

where $\Pi(\theta)$ is the rectangular function of width θ. The height in intensity h_k of each step fulfills the condition $0 \leq h_k \leq h_0$ whatever the wavelength is. This is to avoid solutions having a surrounding environment brighter than a central star.

---

*made freely available at https://github.com/jdrevon/RHAPSODY

Thus, the final expression of the global visibility is:

$$V_{\mathrm{Hankel}}[q, a_k(\lambda)] = \sum_{k=0}^{N_{\mathrm{step}}-1} a_k(\lambda) \; \frac{\theta_{k+1}^2 \; V_{\mathrm{UD}}(q; \theta_{k+1}) - \theta_k^2 \; V_{\mathrm{UD}}(q; \theta_k)}{\theta_{k+1}^2 - \theta_k^2}, \tag{2}$$

where the visibility coefficients a_k, that are varied by our reconstruction method, are:

$$a_k(\lambda) = \frac{h_k(\lambda)}{\sum_{k=0}^{N_{\mathrm{step}}-1} h_k(\lambda)} \tag{3}$$

One can note here the little trick of using uniform disks to represent rings with a non-zero thickness. The visibilities of each uniform disk can be pre-computed initially to save computing time afterwards. A consequence of this trick is the step-like appearance of our radial profiles. A smoother version is in preparation and its description is beyond the scope of this paper.

Adjusting V_{Hankel}^2 to the measured squared visibilities V_{obs}^2 (with their uncertainties σ_{obs}) is then a matter of minimizing the distance between both through a χ^2 minimization, varying the a_k coefficients.

$$\chi^2(\lambda) = \sum_q \frac{\left(V_{\mathrm{Hankel}}^2[q, a_k(\lambda)] - V_{\mathrm{obs}}^2[q]\right)^2}{\sigma_{\mathrm{obs}}^2} \tag{4}$$

However, trying to adjust the visibility deduced from a lot of regular intensity steps using a bare final χ^2 value usually gives poor results, because the number of parameters a_k to fit becomes large compared to the number of available data, in a similar way as in an image reconstruction problem. This is where the Bayesian method comes into play by adding to the simple χ^2 an *a priori* information.

2.3 The Bayesian Approach

This additional information to the problem-solving is called a *regularization* term f_{prior}, calculated on the variable parameters themselves. Such a regularization term must be designed so as to maximize the probability that the reconstructed profile resembles the "true" one. For more details on how to deal with heavy inverse problems in a Bayesian framework, we refer the reader to the excellent introduction to image reconstruction for optical interferometry.[8]

Adjusting the Hankel profile to the visibility data is then a matter of adding the χ^2 and the regularization term f_{prior} multiplied with a so-called *hyper-parameter* μ, that is arbitrarily set:

$$f_{\mathrm{tot}}(\lambda) = \chi^2(\lambda) + \mu \; f_{\mathrm{prior}}(\lambda) \tag{5}$$

In our case, we have tested two different regularization terms for f_{prior}: (1) a *smoothness* term $f_{\mathrm{prior}} = f_{\mathrm{smooth}}$, or (2) a *total variation* term $f_{\mathrm{prior}} = f_{\mathrm{var}}$. On the one hand, the smoothness f_{smooth}, described by the intensity difference between adjacent rings, is given by:

$$f_{\mathrm{smooth}}(\lambda) = \sum_{k=0}^{N_{\mathrm{step}}-1} \sqrt{\left[h_{k+1}(\lambda) - h_k(\lambda)\right]^2}. \tag{6}$$

f_{smooth} will tend to minimize the variations between consecutive radii, resulting into a smooth radial profile. On the other hand, the total variation regularization term f_{var} defined as:

$$f_{\mathrm{var}}(\lambda) = \sum_{k=0}^{N_{\mathrm{step}}-1} \left[\frac{h_{k+1}(\lambda) - h_k(\lambda)}{\theta_{k+1} - \theta_k}\right]^2, \tag{7}$$

will tend to reconstruct uniform intensities with sharp edges. Solving the problem (i.e. finding the right radial profile) consists therefore in minimizing the term in Eq. 5, by varying the parameters a_k using a gradient descent or any other optimization algorithm (in our case: the `Cobyla` minimization routine from the `Lmfit` package [†]

[†]made freely available at https://github.com/lmfit/lmfit-py/

library that can be found in `Python`). This description of the algorithm corresponds exactly to the version of RHAPSODY the has been been used in[9]

2.4 Rotation and Inclination

In order to make progress towards a more versatile image reconstruction tool, we introduced at the occasion of the 2022 interferometric imaging beauty contest the possibility to reconstruct flattened structures (like e.g. disks).

All the transformations are done directly in the Fourier plane with coordinates (u, v). The inclination i is simulated by a $cos(i)$ compression factor along the chosen axis which becomes the major-axis in the Fourier plane (i.e., the minor axis in the image plane).

$$\text{Fourier plane}: \begin{cases} u^{'} = u \\ v^{'} = v/\cos(i) \end{cases} \quad \text{Image plane}: \begin{cases} x^{'} = x \\ y^{'} = y * \cos(i) \end{cases} \tag{8}$$

Then, the rotation is made through a change of coordinate with a position angle θ:

$$\text{Fourier plane}: \begin{cases} u^{"} = u^{'} \sin(\theta) + v^{'} \cos(\theta) \\ v^{"} = -u^{'} \cos(\theta) + v^{'} \sin(\theta) \end{cases} \quad \text{Image plane}: \begin{cases} x^{"} = x^{'} \cos(\theta) + y^{'} \sin(\theta) \\ y^{"} = -x^{'} \sin(\theta) + y^{'} \cos(\theta) \end{cases} \tag{9}$$

2.5 From 1D to 2D Fourier plane and "Image" Reconstruction

To reconstruct a flattened radial profile, we first need to pick the pre-computed visibilities at the right compressed and rotated coordinates. Since before the change of coordinate, we are dealing with angular centro-symmetric structure, all the information which is shrunk by the compression factor and rotated by an angle θ is located inside the 1D visibility curve. Hence, RHAPSODY makes an interpolation at spatial frequencies $q_\theta = \sqrt{u^{"2} + v^{"2}}$ on the 1D visibility curve to get the new visibility points of the inclined and rotated modeled structure. Once we have a complete 2D Fourier plane, the code apply an inverse Fourier transform and retrieve the equivalent structure in the image plane.

3. OUTPUT ROBUSTNESS

Here we test RHAPSODY against simple and more complex models to assess its intrinsic capabilities and limits.

3.1 Uniform Disk

We modeled interferometric data based on multiple uniform disks with different diameter using the ASPRO2 software of the JMMC [‡]. We simulated these uniform disks observations as if they were seen by the VLTI/MATISSE instrument. The aim is double: first to check that RHAPSODY is able to correctly reproduce simple model, and second to reach the limit of the code for a given interferometric data-set. In those simulations, we have selected a hyperparameter of $\mu = 1$. The resolution of the MATISSE instrument in L-band is ranging between 3.6 and 275 mas. The results are shown in figures 1, 2, and 3.

First, we observe that at large scales in Fig. 1, RHAPSODY is able to reproduce the uniform disks up to a ≈ 100 mas radius, the 250 mas uniform disk is not well reproduced by RHAPSODY as we reach the interferometric field of view limit of the instrument.

Figure 2 highlights lower scales that the instrument is able to resolve, we can see that RHAPSODY does reproduce the boundaries of the uniform disk properly. We note the presence of artifacts at low flux, especially for the 10 and 20 mas radius uniform disks.

The last modeling attempt is at lower scales (Figure 3), we can see that even if the theoretical resolution of the instrument is at 3.6 mas, we are still able to reproduce structures up to at least half the resolution of the

---

[‡]made freely available at `http://jmmc.fr/~webmaster/jmmc-html/aspro_page.htm`
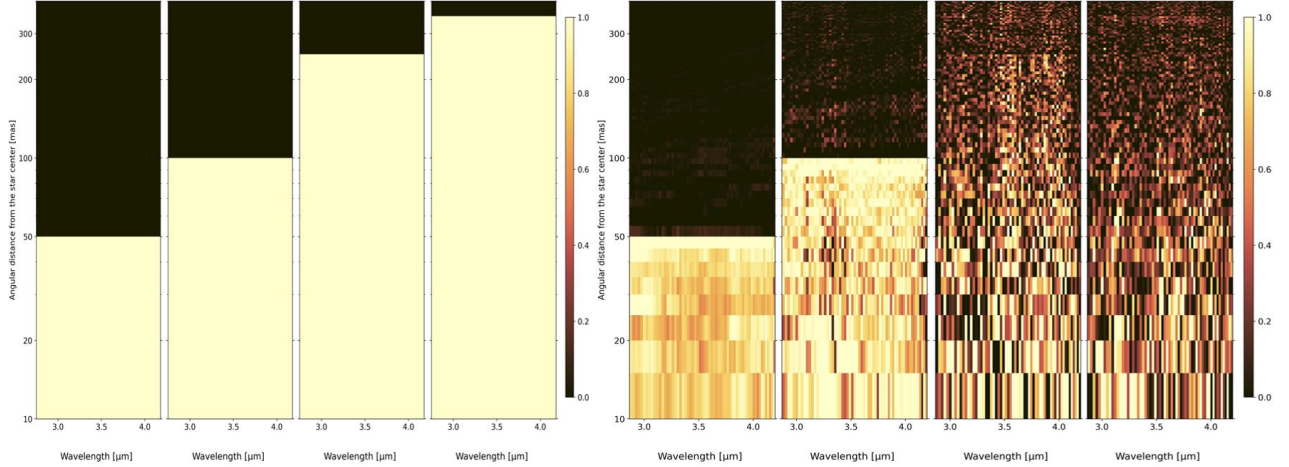
Figure 1: Left Panel: Intensity profile spectra of uniform disk modeled data of respectively a diameter of 100, 200, 500 and 700 mas (50, 100, 250 and 350 mas radius). Right panel: RHAPSODY intensity profile spectra outputs.
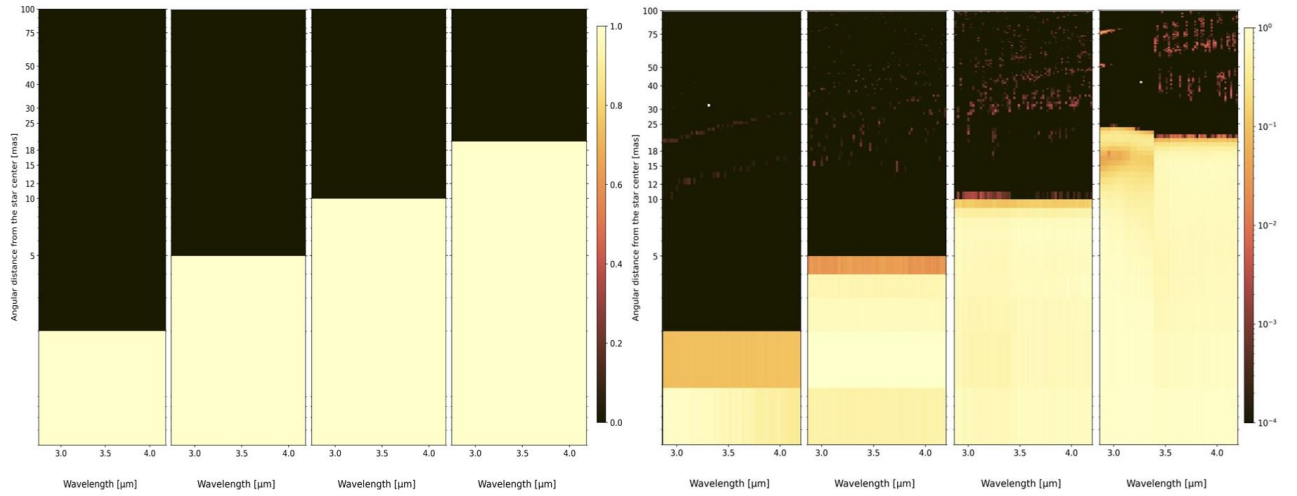

Figure 2: Left Panel: Intensity profile spectra of uniform disk modeled data of respectively a diameter of 4, 10, 20 and 40 mas (2, 5, 10 and 20 mas radius). Right panel: RHAPSODY intensity profile spectra outputs.

instrument. However we remark that the boundaries of the structures are well reproduced, but the shape of the structure is closer to a Gaussian shape than of an uniform disk.

Hence, we can see here the limits of RHAPSODY: At large scales (at or above the interferometric field of view $\lambda/B_{\min}$), the code struggle to proper produce the exact shape of the object, and at small scales, RHAPSODY is still able to get the correct size of the structure up to about half the resolution of the instrument, in a very similar way as for image reconstruction.[8]

3.2 Gaussian Disk

We made a test with an Gaussian model with a 10 mas FWHM in the same way as for uniform disks (Figure 4). We can assert here that a Gaussian model is also generally well reproduced by RHAPSODY.

However, the dynamic range is limited to about 100, as can be seen at the end of the Gaussian wings: at intensities levels between 1% and 0.1% of the peak intensity, the faint reconstructed region starts to exhibit similar artifacts as in Figure 2, hence the flux starts to be poorly spatially constrained.
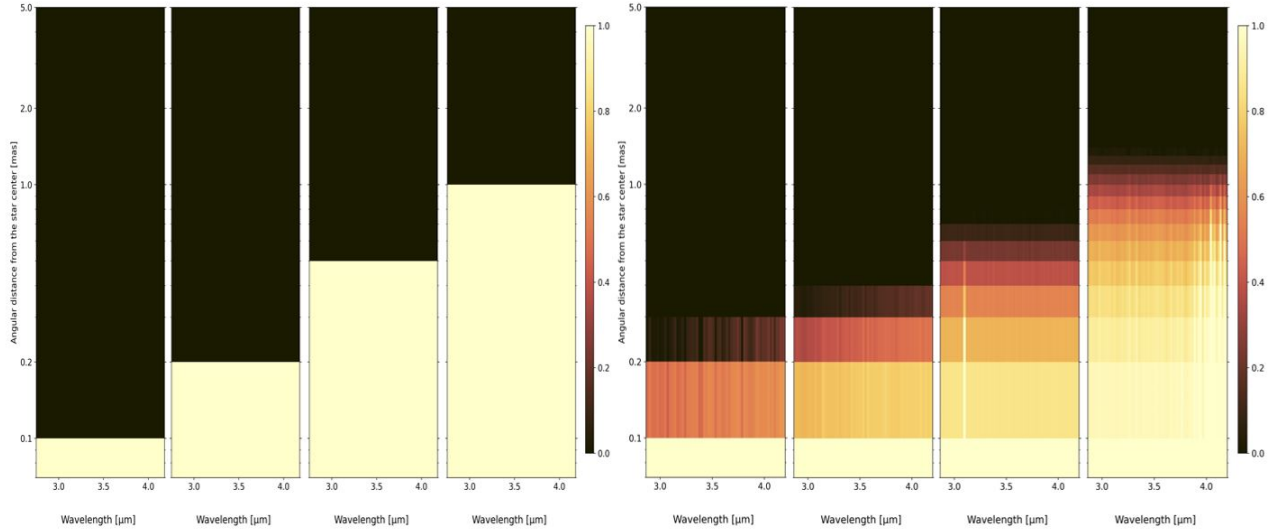
Figure 3: Left Panel: Intensity profile spectra of uniform disk modeled data of respectively a diameter of 0.2, 0.4, 1 and 2 mas (0.1, 0.2, 0.5 and 1 mas radius). Right panel: RHAPSODY intensity profile spectra outputs.
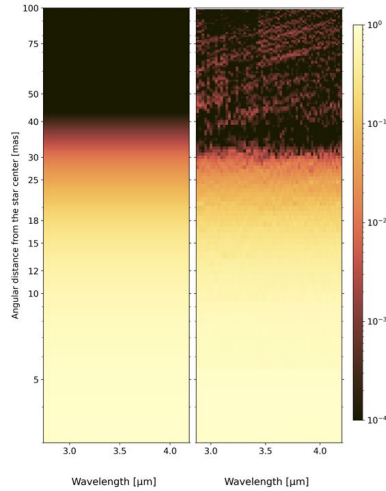

Figure 4: Left Panel: Intensity profile spectra of modeled data of a Gaussian with a FWHM of 10 mas. Right panel: RHAPSODY intensity profile spectra of the same modeled data.

3.3 Elongated Gaussian Ellipse

In this subsection we wanted to test the new feature which bring the 2D aspect of RHAPSODY involving inclination and rotation. We took the same Gaussian disk as in section 3.2 but we added an inclination of 60° and a position angle of 80° and we used RHAPSODY to reconstruct the environment using the modeled interferometric data with ASPRO. The method involved in RHAPSODY allows us to have a face-on description of the object in addition to the reconstructed image produced at the end. As seen in Fig 5, we have successfully reconstructed the Elongated Gaussian Ellipse using RHAPSODY and a hyperparameter of $\mu = 10^3$. The output are the same as the input of our model: as much in terms of the Gaussian FWHM as well as in terms of inclination angle and rotation, with a precision better than 1%.

3.4 1D Dust Radiative Transfer environment

In this paragraph we test the robustness of the RHAPSODY against a realistic model used in our paper on R Scl.[9] We built a toy model mimicking the R Scl environment using DUSTY and a Gaussian layer at 15 mas with an intensity ratio with respect to the central source starting from 1/1000 and reaching up to 1/10 (Fig 8 in appendix).
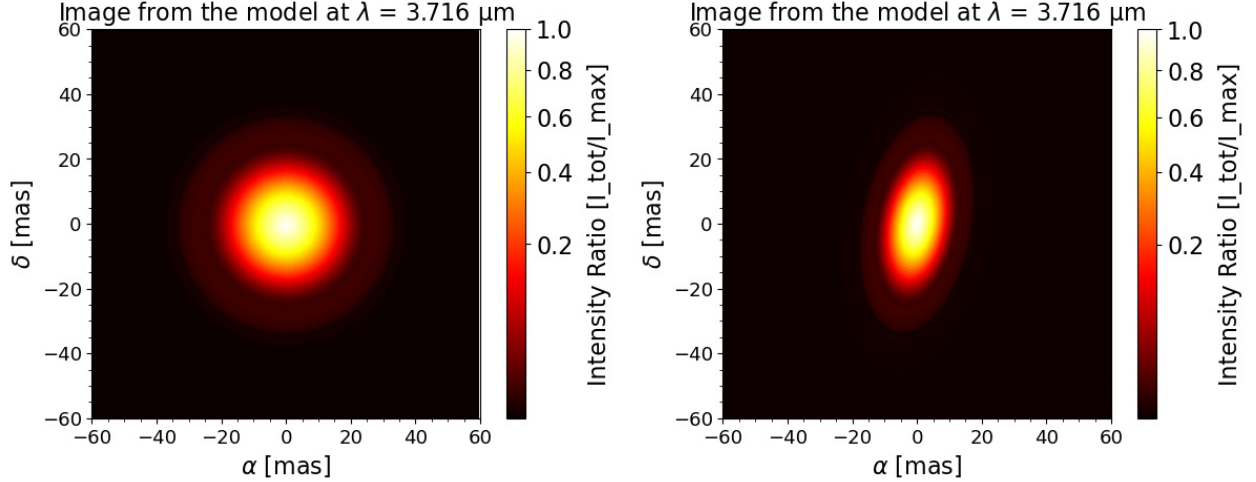
6

Figure 5: Left Panel: RHAPSODY simulations results of the Elongated Gaussian Ellipse with a FWHM of 10 mas, face-on. Right panel: Same RHAPSODY results but as seen by the observer.

Using `ASPRO2`, we generate VLTI/MATISSE visibilities, add error noise to the data, and use the same (u,v)-plane coverage for each of our different models and for both LM- and N-bands.

The initial guess intensity profiles used by `RHAPSODY` for all the simulations in both bands are similar to the one used in this paper (i.e. Gaussian profile with a $FWHM = 7$ mas). The value of the hyperparameter used is $\mu = 1$. Figure. 8 shows the spectra of the intensity profile reconstruction produced by `RHAPSODY`. We can notice that the lower limit of the dynamic range in L-band is about $1/200$ (0.5%). In N-band, the code does not reconstruct (or very marginally) the inner Gaussian structure added at 15 mas whatever its intensity. We suspect this non-detection in N-band is due to an unfortunate combination of instrumental angular resolution and dynamic range.

4. USING RHAPSODY ON REAL AND BENCHMARK DATA

4.1 Spherical envelope: R Sculptoris

R Scl was observed for the first time simultaneously in both L- and N-bands with the VLTI/MATISSE instrument. We used RHAPSODY to analyze this dataset.[9]

Thanks to this tool, we have discovered interesting structures in the vicinity of the star. As we can see in Fig 6, RHAPSODY has spotted two interesting structures in L-band: one between 5 and 7 mas, above the Rosseland radius (dashed blue line) and one between the two green lines between 12 and 18 mas. A layer beyond the estimated Rosseland radius of R Scl is seen as a faint environment between 5 and 7 mas (~ 1.0–$1.3\,R_\star$), assuming that the border of the photosphere is at 5 mas from the center of the star.

Thanks to the spectral information provided by the MATISSE instrument we interpret this layer as a mixture of molecules (C_2H_2 + HCN). In addition, we have spotted another layer at a further distance from the star which could be made of both: dust and molecules.

4.2 Inclined Disk: SPIE Beauty Contest 2022

As seen in Figure 7, we also took the opportunity of this SPIE 2022 conference to participate to the SPIE Beauty Contest 2022. We used a total of 56 rings with a 2 mas width, we have a total of 616 parameters for the 11 wavelengths involved in RHAPSODY. We added two parameters in our algorithm: flattening and position angle on the plane of the sky, for each wavelengths, leading to a total of 638 parameters for 1440 visibility points. Hence, the number of parameters is inferior to the number of measurements.

We applied it to the first set of the beauty contest "contest1". The RHAPSODY images show a bright central source surrounded by an elongated 8.5 mas radius (major axis) ring with a flattening ranging from 0.6 to 0.7.
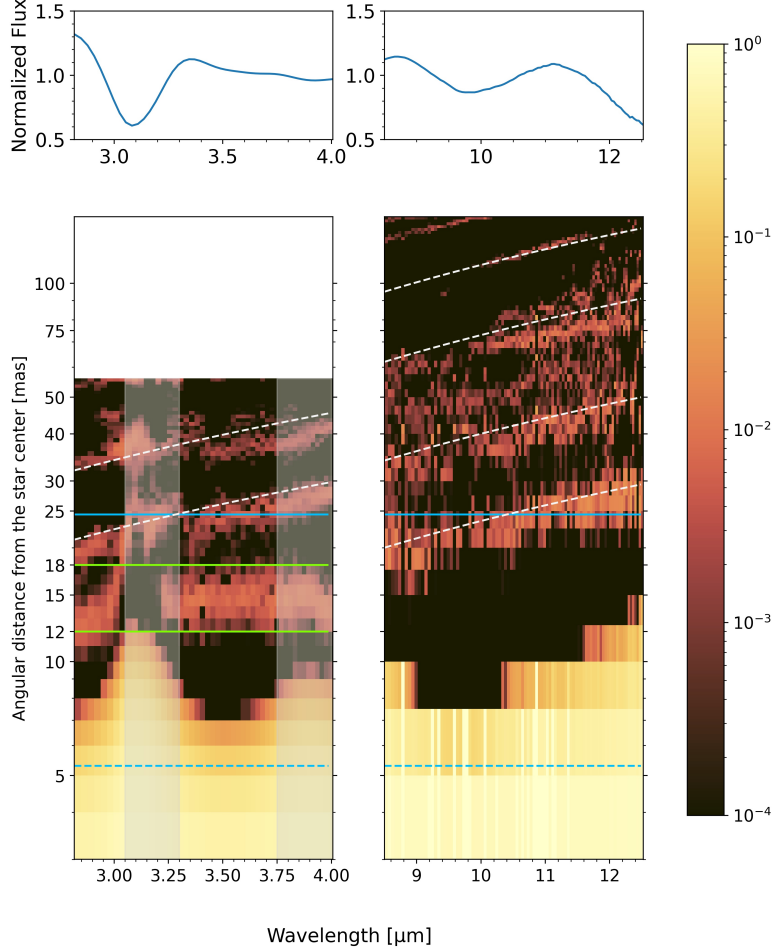
Figure 6: Upper panels correspond to the observed MATISSE spectrum normalized by the median and then divided by a black body spectra at T=2700 K to underline the observed emission and absorption features. Lower panels are the spectro-radial maps in L- and N-band obtained by plotting the best intensity Hankel profile normalized at one for each observed wavelength. The faint red structures highlighted with the inclined dashed-white lines are reconstruction artifacts). The dashed and solid blue horizontal lines show the position of the Rosseland radius and the DUSTY inner radius respectively. The solid green horizontal lines delimit the extension of a hot distinct molecular layer). The grey vertical bands cover the spectral ranges where the centro-symmetric Hankel profile is not able to properly reproduce the asymmetric shape of R Scl revealed by non-zero closure phases.

We can compute an inclination of that ring, that ranges from 45 to 50°, corresponding to the inclination angle of a disk if that structure were indeed a thin disk. The disk position angle ranges from 41 to 55°. The central source seems to be resolved or partially resolved.
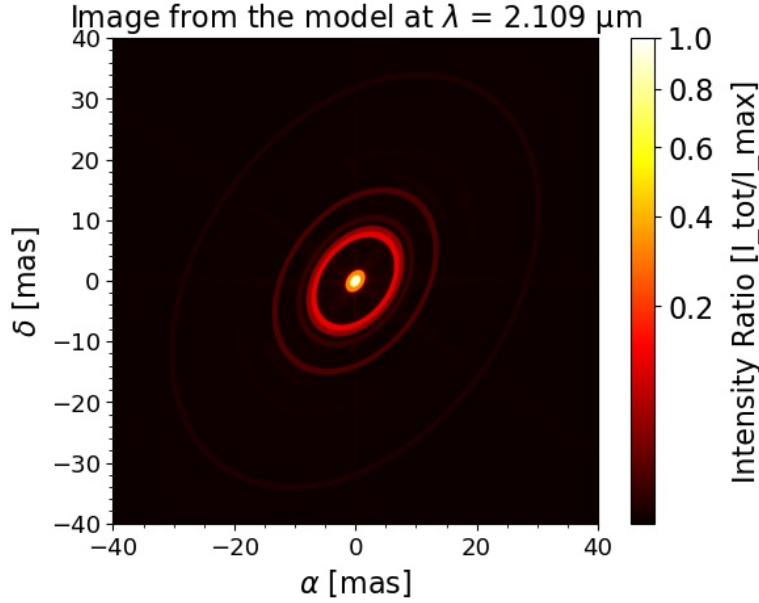
ACKNOWLEDGMENTS

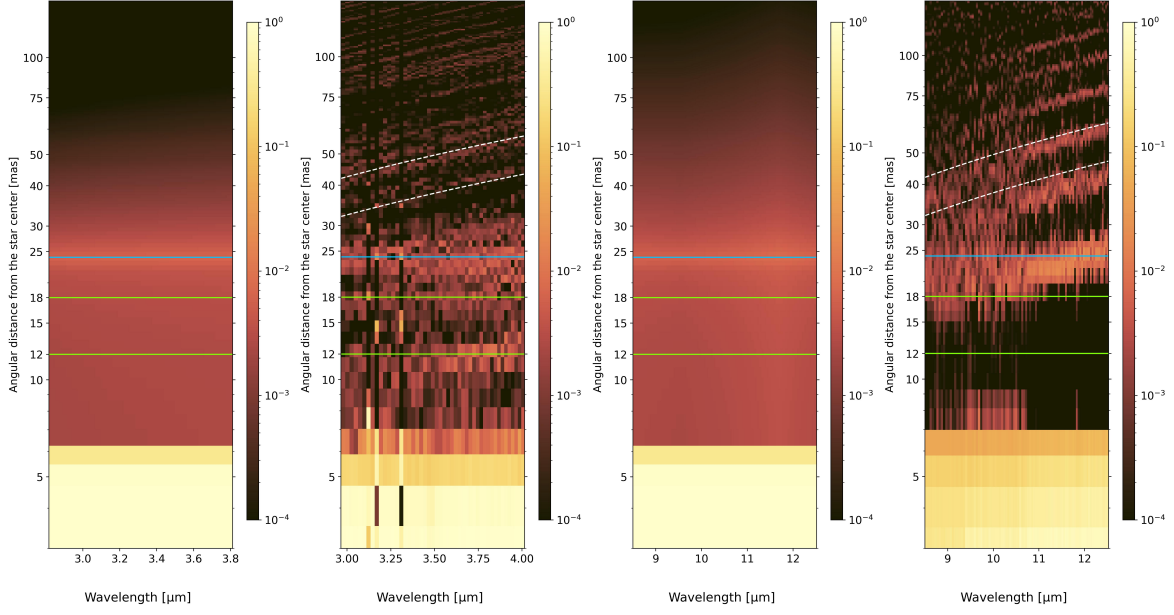Figure 7: RHAPSODY contribution to the SPIE 2022 beauty contest.

tools to prepare this paper. We can cite among others ASPRO[§] used to prepare the modeled data.
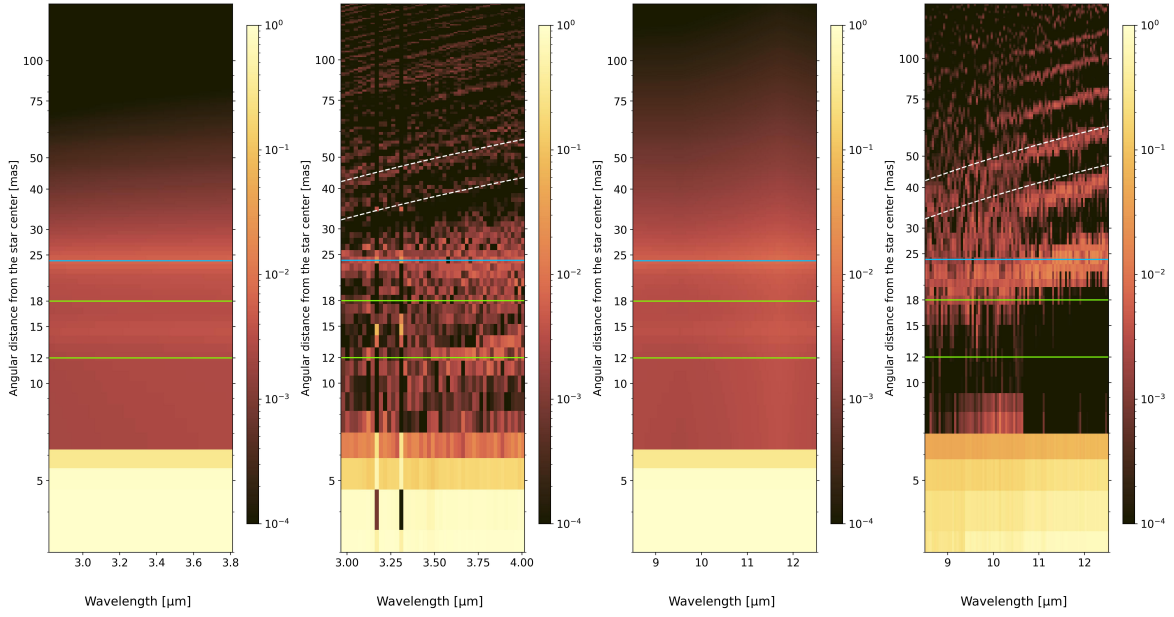
REFERENCES

[1] Buscher, D. F., "Direct maximum-entropy image reconstruction from the bispectrum," in [*Very High Angular Resolution Imaging*], Robertson, J. G. and Tango, W. J., eds., **158**, 91 (Jan. 1994).

[2] Malbet, F., Cotton, W., Duvert, G., Lawson, P., Chiavassa, A., Young, J., Baron, F., Buscher, D., Rengaswamy, S., Kloppenborg, B., Vannier, M., and Mugnier, L., "The 2010 interferometric imaging beauty contest," in [*Optical and Infrared Interferometry II*], Danchi, W. C., Delplancke, F., and Rajagopal, J. K., eds., **7734**, 966 – 977, International Society for Optics and Photonics, SPIE (2010).

[3] Hofmann, K. H., Weigelt, G., and Schertl, D., "An image reconstruction method (IRBis) for optical infrared interferometry," *A&A* **565**, A48 (May 2014).

[4] Millour, F., "Hot Stars and Interferometry," in [*Revista Mexicana de Astronomia y Astrofisica Conference Series*], Revista Mexicana de Astronomia y Astrofisica Conference Series **38**, 1–4 (Feb. 2010).

[5] Claes, R., Kluska, J., Van Winckel, H., and Min, M., "Neural network based image reconstruction with astrophysical priors," in [*Society of Photo-Optical Instrumentation Engineers (SPIE) Conference Series*], Society of Photo-Optical Instrumentation Engineers (SPIE) Conference Series **11446**, 114461U (Dec. 2020).

[6] Sanchez-Bermudez, J., Thiébaut, E., Hofmann, K.-H., Heininger, M., Schertl, D., Weigelt, G., Millour, F., Schutz, A., Ferrari, A., Vannier, M., Mary, D., and Young, J., "The 2016 interferometric imaging beauty contest," in [*Optical and Infrared Interferometry and Imaging V*], Malbet, F., Creech-Eakman, M. J., and Tuthill, P. G., eds., **9907**, 372 – 389, International Society for Optics and Photonics, SPIE (2016).

[7] Duvert, G., Young, J., and Hummel, C. A., "OIFITS 2: the 2nd version of the data exchange standard for optical interferometry," *A&A* **597**, A8 (Jan. 2017).

[8] Thiebaut, E. and Giovannelli, J. F., "Image reconstruction in optical interferometry," *IEEE Signal Processing Magazine* **27**, 97–109 (Jan. 2010).

[9] Drevon, J., Millour, F., Cruzalebes, P., Paladini, C., and Hron, J. e., "Locating dust and molecules in the inner circumstellar environment of R Sculptoris with MATISSE," *A&A* (2022).
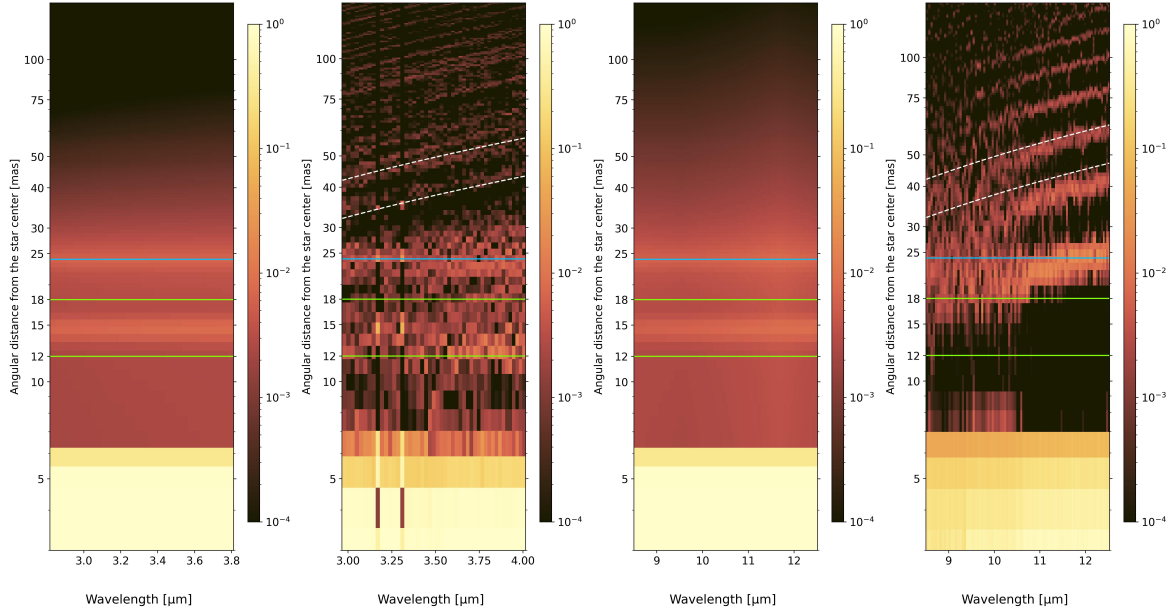
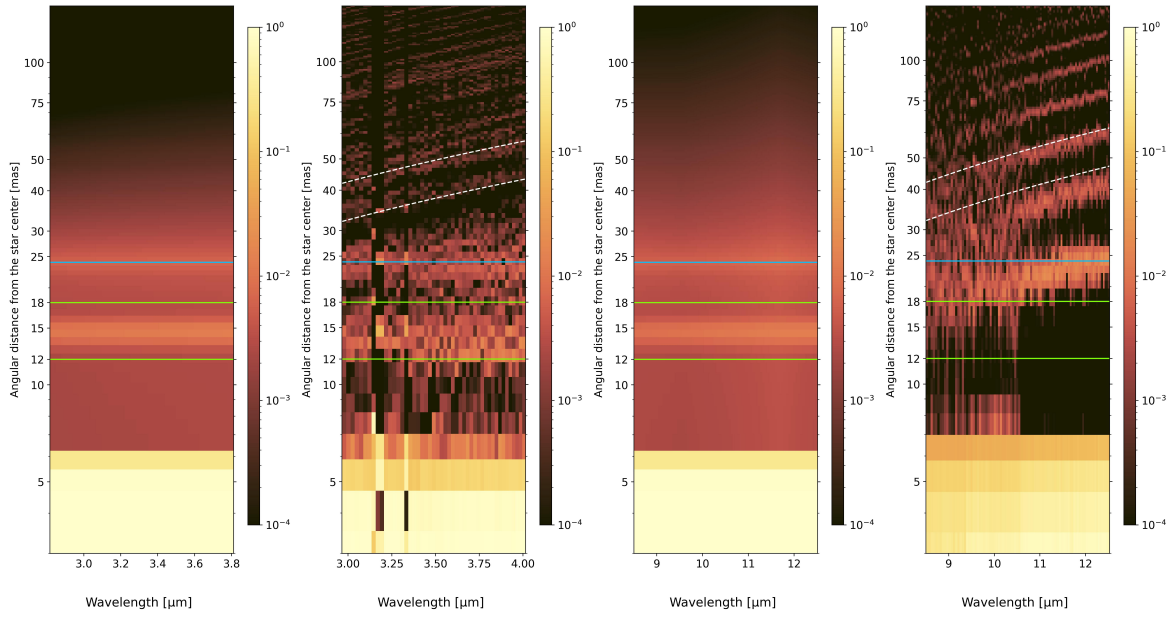(a) Without the gaussian layer at 15 mas

(b) Additional gaussian layer at 15 mas with an intensity ratio with respect to the star of 1/1000
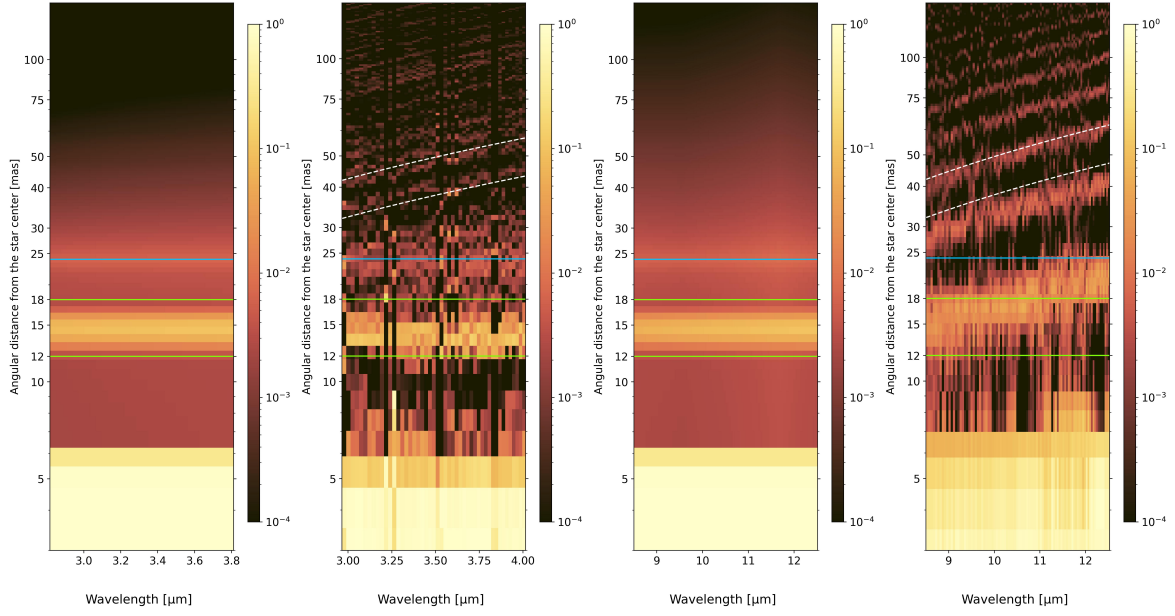
Figure 8: Top view continued...

(c) Additional gaussian layer at 15 mas with an intensity ratio with respect to the star of 1/200

(d) Additional gaussian layer at 15 mas with an intensity ratio with respect to the star of 1/100

Figure 8: Top view continued...

11

(e) Additional gaussian layer at 15 mas with an intensity ratio with respect to the star of 1/10

Figure 8: Modeled intensity spectra from DUSTY panels 1 and 3 and its associated RHAPSODY intensity profiles reconstruction spectra 2 and 4 in L-Band and N-band respectively (from left to right). A gaussian layer has been also added at 15 mas with an intensity ratio comparing to the star of 1/1000, 1/200, 1/100, 1/50, 1/20, and 1/10.